Anode Plasma Influence on Breakdown Formation in Explosive-Emission Electron Sources

E.N. Abdullin, G.P. Bazhenov, and A.V. Morozov

Institute of High Current Electronics, 2/3, Akademichesky ave., Tomsk, 634055, Russia
Phone: 8(3822) 49-19-13, Fax: 8(3822) 49-24-10, E-mail: abdullin@lhfe.hcei.tsc.ru

Abstract – Breakdown formation in the explosive-emission sources is related to the interelectrode gap filling with the cathode and anode plasma generated at the anode and in the gap under the beam influence. Under conditions of saturation of the cathode plasma emissive ability as well as when the measures on the emission boundary stabilization are taken, the anode plasma has the deciding part in the formation of the electron source breakdown. The paper presents the results of the anode plasma investigations obtained at solving the problem of the electron beam length increase in the explosive-emission sources. The data concerning the gas release from the anode, the mechanism of the anode plasma formation and the anode plasma influence on the parameters of the generated electron beam are presented as well.

1. Introduction

Breakdown formation in explosive-emission electron sources is related to the growth of the interlelectrode gap conductivity resulting from filling with cathode and anode plasma. At high beam current densities, the time preceding the anode plasma appearance is short and the interelectrode gap conductivity grows rapidly. The rate of the interelectrode filling with the interelectrode gap plasma calculated from the values of the diode perveance can exceed $2 \cdot 10^6$ cm/s at the beam length being equal to ~ 10^{-7}–10^{-6} s.

At the decrease of the current and beam current density, the current distribution along a large number of emission centers, the time preceding the anode plasma appearance is increased and here the cathode and anode plasma influence on the rise of the interelectrode gap conductivity can be divided. Under these conditions, the rate of the cathode plasma propagation is decreased owing to saturation of the plasma emissive ability and discharge transition into a quasistationary phase. Anode plasma appearance results in discharge transition into a high-current phase characterized by a rapid rise of the gap conductivity completed with the ignition of a low-voltage arc discharge that testifies to an important role of the anode plasma in the electron source breakdown formation. The time length of a high-current phase of the discharge makes up ~ 10^{-6} s.

Earlier it was shown that the main process responsible for anode plasma generation is the gas release from the anode under the electron beam action. Gas release has a desorption nature and is not related to the thermal action of the beam. Gas release efficiency was ranging from 2–3 to 10 molecule/electron at the electron energy ranging from 10–20 to 100 keV [1]. The time preceding the anode plasma generation is in inverse proportion to the beam current density at the anode. Increase of the beam current density results in the growth of the time preceding the discharge transition into a high-current phase that can be related to the exhaustion of the adsorbed gas films in the discharge process.

The paper presents the data concerning a mechanism of the anode plasma influence on the breakdown generation in the interelectrode gap, estimates a contribution of radiolysis in the organic contamination films and condensed vapor of the pump fluid in the process of gas release from the anode.

2. Anode plasma influence on the interelectrode gap processes

The data concerning the influence of anode processes on the breakdown generation in the interelectrode gap with the explosive-emission cathode have been obtained by means of a complete factorial experiment fulfilled by the plan 23 [2]. The cathode (C), anode (A) and interelectrode gap (G) processes were considered as the main ones. The cathode processes imply the processes of the cathode plasma generation, cathode erosion, electron emission supply. The anode processes are related to the changes at the anode in the process of current flowing. The interelectrode gap processes implied the processes resulting in the change of its conductivity. Full set of processes in the interelectrode gap included the following interactions: A×C, A×G, G×C, A×G×C (Fig. 1). Commutation time tc, corresponding to the time preceding the discharge transition into an arc stage, was taken as an integral characteristic. Ranking of processes by their contribution into t_c was realized by Fisher significance test.

The experiment consisted in supplying a stepwise pulse with the first step amplitude of 35 kV to the interelectrode gap with a pointed cathode and plane anode that provided a stable initiation of emission. The second stage amplitude equaled to 2 kV and was chosen from condition of reliable sustaining of the discharge after voltage dropping. Intensity of the processes varied at two discrete levels. The first step pulse length being equal, correspondingly, to 10 ns at the lower level and 300 ns at the upper level, served as the

intensity measure of C-processes. A gap with the anode in the form of a grid with geometrical transparency of 0.9 corresponded to the lower level and a gap with a solid anode corresponded to the upper level.

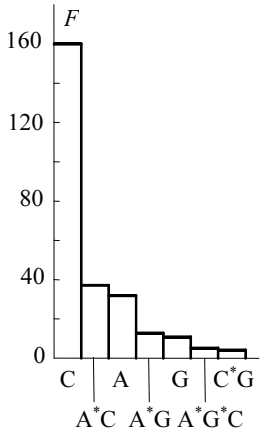

Fig. 1. The pattern of a set of discharge processes and their significance

A residual gas pressure of $5 \cdot 10^{-5}$ mm Hg and $2 \cdot 10^{-3}$ mm Hg corresponded, respectively, to the lower and upper levels of G-processes. Combinations of intensities are indicated in Table 1 being a design matrix. Minus sign corresponds to the lower levels of factors, and plus sign, respectively, to the upper levels. Values of tc were determined as a mean value by 10 measurements. Calculation values of Fisher criterion are presented in the fifth column of the Table 1 and in Fig. 1. The standard value of *F*-criterion at a 5% significance level and numbers of degrees of freedom $f_1 = 1$ and $f_2 = 72$ is equal to 4.

Table 1. Design matrix 23

C	G	A	t_c, μs	*F*
–	–	–	3.52	
+	–	–	2.66	161
–	+	–	2.62	10.4
+	+	–	2.42	3.9
–	–	+	3.10	31.9
+	–	+	1.60	36.9
–	+	+	3.16	12.5
+	+	+	1.64	4.4

As it follows from comparison of the calculation value of *F*-criterion with the standard one, only C×G-interaction is insignificant.

The above presented data show that the main processes responsible for conductivity rise and generation of interelectrode gap breakdown are C-processes that is related to the cathode plasma generation and expansion into the interelectrode gap.

Anode influence on breakdown generation becomes apparent in A-processes, A×C- and A×G-interactions being, correspondingly, the third, the second, and the fourth by significance.

At the low beam current densities (10^{-2}–10 A/cm^2), the main anode processes responsible for discharge development are gas release from the anode and anode plasma generation. High significance of A×C-interaction is related to a characteristic feature of explosive-emission sources consisting in dependence of the cathode plasma emissive ability on the current value. Owing to the back-coupling between the current value, emissive ability and anode plasma concentration, the growth of current related to the anode plasma initiation results in the termination of saturation and cathode plasma propagation towards the anode providing fast increase of the interelectrode gap conductivity. Use of artificially created anode plasma with constant concentration in the plasma-filled diodes [3] as well as other measures allowing reducing A×C-interaction results in deceleration of the interelectrode gap conductivity growth and increase of duration of a high-current discharge phase up to ~ 10^{-5} s.

3. Anode plasma influence on electron beam parameters

Anode plasma appearance in the vacuum diode results in limitation of duration of a quasistationary discharge phase and, correspondingly, electron beams generated in the discharge.

Depending on the current density, two variants of anode plasma generation are possible. At the small densities of the beam current being of ~ 10^{-2} A/cm^2 and less and large durations of the beam being of ~ 10^{-4} s and larger, a concentration behind the desorbed gas has a small difference with the residual gas one. As a result, beam generation is accompanied with gradual pressure increase in the whole volume of the interelectrode gap. The value of the critical pressure corresponding to the plasma generation resulting in the discharge arc ignition in the interelectrode gap is found from the ratio [4]

$$\sqrt{\frac{M}{m}} n_{cr} \sigma d \frac{I}{U} = 0.221 \quad . \tag{1}$$

Here, *M* and *m* are the ion and electron masses, correspondingly, σ is the ionization section, *d* is the interelectroge gap, *I* is the ionization potential, *U* is the applied voltage.

At the current densities ranging from 0.1 to 10 A/cm^2 and higher, the concentration behind the desorbed gas leading edge exceeds essentially the residual gas one resulting in plasma generation in the gas layer prior to the moment when the gas leading edge achieves the cathode surface. The time preceding the plasma generation t_0 is found from the ratio [5]

$$t_0 = \sqrt{\frac{m}{M}} \frac{e}{\gamma \sigma} \frac{1}{j_e} . \tag{2}$$

Here, j_e is the beam current density, *e* is the electron charge, γ is the desorption efficiency.

For $M \sim 13$, $\gamma = 10$, $\sigma = 10^{-17}$ cm^2 (ionization section with electrons of the energy 10^5 eV), the following ratio will be obtained from (1)

$$t_0 = \sqrt{\frac{m}{M}} \frac{e}{\gamma\sigma} \frac{1}{j_e} \qquad (3)$$

Figure 2 presents the diagram of the dependence $t_0(j_e)$ from (3). The values of duration of a quasistationary discharge phase in the electron sources with multipointed cathodes at relatively small current densities (~ 1 A/cm^2) are indicated here as well. It is seen that the calculation values are close to the experimental ones.

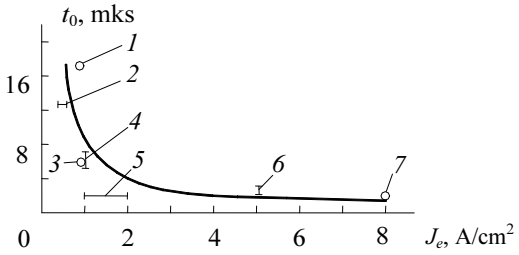

Fig. 2. Dependence (3) and value of t_0 according to reference data (*1* – [6]; *2* – [7]; *3*, *7* – [8]; *4* – [9]; *5* – [10]; *6* – [11])

Current density enlargement results in a certain increase of a quasistationary phase duration and partial beam compression under the action of a self-magnetic field.

$$t_0 = \frac{2\times10^{-5}}{j_e} \qquad (3).$$

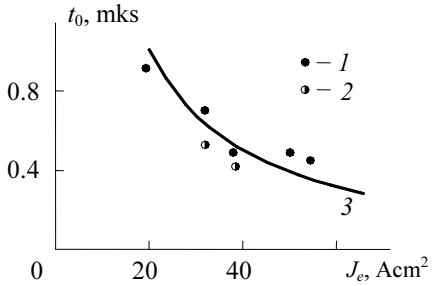

Fig. 3. A quasistationary phase duration in a diode with a felt (*1*) and velvet (*2*) covering and dependence

Figure 3 presents the duration of a quasistationary discharge phase versus current density for a diode with velvet-covered or carbon-felt-covered cathodes [12]. Use of coverings provides the current distribution over a large number of emission centers promoting obtaining of a sufficiently defined quasistationary discharge phase. Duration of the quasistationary discharge phase is approximately inversely proportional to the current density. However, the time preceding the fast growth of the diode perveance turns out to be larger than the one obtained at small current densities that results in the constant reduction in the dependence of $t_0(j_e)$ in (3) from $8 \cdot 10^{-6}$ to $2 \cdot 10^{-6}$ s. The reasons can be related to the decrease of the gas release to $\gamma = 4$–5 owing to a high degree of anode degassing and exhaustion of adsorbed films at high current density.

Reduction of the anode plasma influence on the processes in the interelectrode gap with current density increase was observed in the electron accelerator with an electron energy of 500–550 keV, beam current of 50–70 kA, cross-section of $25 \cdot 100$ cm^2 [13]. Anode plasma generation resulted in the diode current increase in comparison with the values obtained from numerical calculations in the absence of anode plasma and beam compression to the diode symmetry plane. The accelerating voltage increase accompanied by enlargement of the beam current density resulted in decrease of exceeding of the experimental current values over the calculated ones that testified to the decrease of the desorbed gas influence on the interelectrode gap conductivity. The causes of decrease, just like in the previous case, can be exhaustion of adsorbed gas films, higher degree of anode degassing at high beam current densities.

4. Gas release mechanism

Values of the gas release efficiency from the anode exceed essentially the well-known values of efficiency of electron-stimulated desorption equal ~ 10^{-2} molecule/electron. In view of this, a possibility of gas release from the anode resulting from radiolysis in condensed vapor films of pump fluid and organic contaminations was considered [14].

Presence of large volumes of condensed vapors of pump fluid at the electrodes in vacuum is well known.

According to [15], an oil (VM-1) film of the thickness ~ 10^3 Å is formed at the electrodes during several hours of pump operation in the systems pumped with vapor-oil pumps in the absence of freezing out catchers.

It is well-known that the main radiochemical reactions in condensed medium take place in local regions, spur dikes wit the transverse diameter of ~ 10 Å where a preferential liberation of bombarding electron energy occurs. The energy absorbed in the region of a spur dike is spent mainly for ionization and makes up 50–100 eV. For the electrons with an energy of ~10^5 eV the value of losses in the organic film can be taken as ~ 5 MeV/cm. Then the distance between the spur dikes is equal to ~ 103 Å that is commensurable with the film thickness.

Radiochemical reaction results in formation of a strong polymer film at the surfaces under radiation. The main gases being released are hydrogen, hydrocarbons. The value of radiochemical release of the gas is 3–5 molecule/100 eV of the absorbed energy [16]. Account of reflected electrons results in increase of the released gas quantity.

The value of the released gas flow is limited by the gas diffusion from the film volume. For the case of the

electron beam with a large cross-section, disregarding the time of radiolysis (~ 10^{-8}–10^{-7} c), the diffusion equation is the following:

$$\frac{\partial n}{\partial t} = D\frac{\partial^2 n}{\partial x^2} + a\frac{J_e}{e}G\varepsilon. \quad (4)$$

Here, n is the gas concentration in the film, D is the diffusion coefficient, a is the coefficient taking into account the growth of gas release resulting from inelastic reflection of the beam electrons, G is the radiochemical release of the gas, ε is the value of ionization losses. Boundary and initial conditions are the following:

$$n_{x=0} = 0; \frac{\partial n}{\partial t_{x=l}} = 0; \; n_{t=0} = 0.$$

According to [17], the solution of equation (1) looks like:

$$n(x,t) = (a\frac{j_e}{e}G\varepsilon)\frac{2}{lD}\sum_{k=l}^{\infty}\left(\frac{2l}{\pi k}\right)^3\left[1 - e^{-\left(\frac{\pi k}{2l}\right)^2 Dt}\right]\sin\frac{\pi k}{2l}x. \quad (5)$$

The time for setting the equilibrium concentration of the gas τ depends on the film thickness l. Limiting ourselves to the first term of series, obtain

$$\tau = \frac{l_2}{D}. \quad (6)$$

According to [18], a diffusion coefficient in cm^2/s in liquid is

$$D = 7.4\cdot 10^{-8}\left[\sqrt{FM_2T/\mu_2 V_1^{0.6}}\right]. \quad (7)$$

Here, M_2 is the molecular mass of a solvent; T is the temperature, K; μ_2 is the solvent viscosity, cP; V_1 is the molar volume of a solute, cm^3/mole; F is the parameter ($F \sim 1$). For a diffusion oil film (μ_2 = 65 cP at 50 ºC, M_2 ~1000) and V_1 = 14–30 for H_2, O_2, CO [16], obtain that $D \approx 3 \cdot 10^{-6}$ cm^2/s. For a film with a thickness of $l = 10^3$ Å, find that $\tau \approx 3 \cdot 10^{-5}$ s. Since viscosity value of a viscous fluid decreases rapidly with the temperature growth, the heating of the surface under radiation results in additional decrease of τ. Under conditions of steady concentration, the flow of the released gas is proportional to the electron current density:

$$j_D = a\frac{j_e}{e}Gl\varepsilon. \quad (8)$$

For $a = 2$, $G = 3 - 5$, $l = 10^{-5}$ cm, ε = 5 MeV/cm, find that the value of gas release efficiency is $\gamma = aGl\varepsilon$ = (3–5) molecule/electron that is close to the values obtained in [1].

References

[1] E.N. Abdullin and G.P. Bazhenov, Zh. Tekh. Fiz. **51**, 1969 (1981).

[2] E.N. Abdullin, G.P. Bazhenov, G.P. Erokhin, V.N. Kiselev, O.B. Ladyzhensky, and S.M. Chesnokov, *in Proc. 5th All-Union Symp. on High Current Electronics*, 1984, part 1, pp. 255–257.

[3] E.N. Abdullin, G.P. Bazhenov, G.P. Erokhin, and O.B. Ladyzhensky, Pis'ma Zh. Tekh. Fiz. **10**, 257 (1984).

[4] M.A. Zavyalov, Elecktronnaya Obrabotka Materialov, No. 4 (46), 56 (1972).

[5] E.N. Abdullin, G.P. Bazhenov, S.P. Bugaev, and G.P. Erokhin, *in Proc. 4th All-Union Symp. on High Current Electronics*, 1982, part 1, pp. 90–93.

[6] E.N. Abdullin, G.P. Bazhenov, S.P. Bougaev, S.M. Chesnockov, and O.B. Ladyzhenski, *in Proc. 7th ISDEIV*, 1976, pp. 379 – 382.

[7] V.A. Burtsev, M.A. Vasilevsky, A.O. Gusev, A.B. Efimov, I.M. Roife, E.V. Seredenko, and V.I. Engel'ko, Zh. Tekh. Fiz. **48**, 1494 (1978).

[8] E.N. Abdullin, I.N. Konovalov, V.F. Losev, V.F. Tarasenko, and S.M. Chesnokov, Zh. Tekh. Fiz. **52**, 923 (1982).

[9] M.A. Vasilevsky, I.M. Roife, and V.I. Engel'ko, Zh. Tekh. Fiz. **51**, 1183 (1981).

[10] B.M. Kovalchuk, V.A. Lavrinovich, V.I. Manylov, G.A. Mesyats, and A.M. Rybalov, Pribori i Tekh. Eksp., No. 6, 125 (1976).

[11] E.N. Abdullin, V.G. Azarov, and S.P. Bugaev, Zh. Tekh. Fiz. **46**, 2459 (1976).

[12] E.N. Abdullin, V.M. Zaslavsky, and S.V. Loginov, Zh. Tekh. Fiz. **61**, 207 (1991).

[13] E.N. Abdullin, S.Ya. Belomytsev, S.P. Bugaev, S.I. Gorbachev, V.M. Zaslavsky, V.B. Zorin, B.M. Kovalchuk, S.V. Loginov, Yu.N. Matyukov, R.M. Rasputin, V.S. Tolkachev, and P.M. Schanin, Fiz. Plasmy **17**, 741 (1991).

[14] E.N. Abdullin and G.P. Bazhenov, Izv. Vuzov. Fizika, No. 11 (1984), Deposited in VINITI, No. 5616-84.

[15] N.M. Baryshova, Pribori i Tekh. Eksp., No. 6, 139 (1965)

[16] Radiation influence on organic materials, Atomizdat, 1965.

[17] A.N. Tikhonov and A.A. Samarsky, Mathematical physics equations, Nauka, 1972.

[18] P. Rid and T. Sherwood, Gas and liquid properties, Chemistry, 1971.